ISBN: 978-3-95450-227-1 ISSN: 2673-5490 doi:10.18429/JACoW-IPAC2022-MOPOTK031

10 TeV CENTER OF MASS ENERGY MUON COLLIDER

K. Skoufaris*, C. Carli, D. Schulte
European Organization for Nuclear Research (CERN), Geneva, Switzerland

Abstract

A Muon collider can provide unique opportunities in high-energy physics as an energy frontier machine. However, a number of challenges have to be addressed during the design process primarily due to the short lifetime of muons. In this work, a lattice for a 10 TeV center-of-mass energy collider is presented. Some of the more important challenges faced are: the design of an interaction region with β^* values of the order of a few millimeters and an adequate chromatic compensation without sacrificing the physical and dynamic aperture, the flexibility to control the momentum compaction factor and the radiation generated where neutrinos from muons decays reach the surface. These issues are addressed with the development of a new chromatic correction scheme, the extensive use of flexible momentum compaction factor cells and the efficient control of the optical parameters.

INTRODUCTION

Although CERN's Large Hadron Collider (LHC) [1] and its High Luminosity upgrade (HL-LHC) [2] will continue collecting experimental data until the beginning of the forties (Run 5), the new long-term strategy for the field is prepared. Thus, different new collider projects, which could be constructed after the LHC era, the IMCC [3], the FCC [4] and the CLIC [5] are performing their feasibility studies and exploring their capability to discover new physics.

The future colliders are either steered to develop precision machines (use of fundamental particles) or to reach high energy (multi-TeV) collisions to probe the energy frontier. Given that muons are fundamental particles and about 200 times heavier than electrons (less energy losses due to synchrotron radiation), the muon colliders could provide high precision physics measurements at multi-TeV collision energies. The idea of using muons is not new and it was initially discussed in [6]. The present study shows the current status of the 10 TeV collider building blocks (interaction region, chromatic correction scheme and arcs) and is based on former works [7–9].

COLLIDER RING DESIGN

An illustration of the muon accelerator complex can be seen in Fig. 1 while in Table 1 the main parameters of the collider ring are shown. Many challenges of a muon collider [10] are related to the short lifetime of the muons ($\tau_0 \approx 2.2$ s) and the radiation generated from their decay process ($\mu^+ \rightarrow \overline{\nu}_\mu + \nu_e + e^+$ and $\mu^- \rightarrow \nu_\mu + \overline{\nu}_e + e^-$). Due to this unstable nature of muons, the cooling and acceleration stages should perform fast while the collider circumference must be kept short requiring the use of high magnetic fields. The

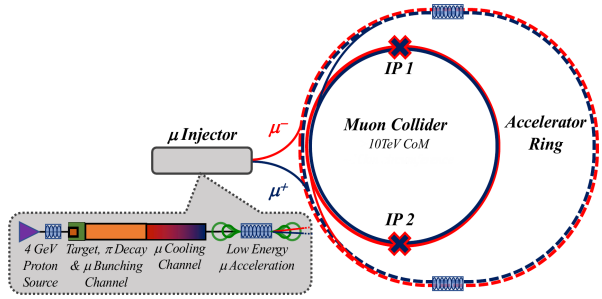

Figure 1: A conceptual scheme of the muon collider complex.

heat load and radiation driven by the muons decay can cause damage around the whole circumference of the collider. Additionally, the muons decaying around the interaction region (IR) generate an intense beam-induced background (BIB) at the detectors which is primarily formed by the secondary and tertiary interactions of the decay products. In order to mitigate the BIB (improve the accuracy of physics measurements), techniques like the addition of nozzles [11] right before and after the interaction point (IP) and special designs of the final focusing (FF) scheme are needed. Another issue from the decay of muons is the neutrino radiation. The large amount of muons used in the bunches ($N_p = 1.8 \times 10^{12}$), generates a large number of neutrinos which reach the earth surface far away from the decay within a small region. The cross section for interaction between these neutrinos and matter is such that the earth does not act as shield thus, mitigation measures are needed to keep doses below legal limits. One such measure is to avoid sections without deflection outside the IR by using combined function magnets (dipole plus a higher order multipole) for focusing and chromatic corrections and limiting straight sections to 30 cm. As a result of the extensive use of dipole fields, the collider ring has a similar shape with a racetrack where the two IRs and any insertion devices are located at the two straight sections.

In order to retain the high precision for physics discovery, the 10 TeV center of mass energy ($\sqrt{s} = 10$ TeV) muon collider ring aims to produce integrated luminosity equal to 10 ab^{-1}. In favor of the high luminosity production, only two high intensity bunches ($N_p = 1.8 \times 10^{12}$) of μ^+ and μ^- will be injected at a time and two interaction points (IPs) with very small β^* values ($\beta^*_x = \beta^*_y = 1.5$ mm) and zero crossing angle will be used. The small β^* values in combination with the large energy spread ($p_T = 0.1\%$) and the lack of a radio frequency system (RF) for longitudinal stability (due to excessive RF voltages and very high frequencies needed) requires a good control of the chromatic phenomena (linear and non-linear ones). A modest RF system without particular contsraints on the frequency is needed to compensate

* kyriacos .dot. skoufaris .at. cern .dot. ch

ISBN: 978-3-95450-227-1 ISSN: 2673-5490 doi:10.18429/JACoW-IPAC2022-MOPOTK031

synchrotron radiation losses, but will not be described in detail.

Table 1: 10 TeV Center of Mass Energy Muon Collider

Parameters	Symbol	$\sqrt{s}$ = 10 TeV
Particle energy [GeV]	E	5000
Luminosity [10^{34} cm^{-2} s^{-1}]	$\mathscr{L}$	20
Bunch population [10^{12}]	N_p	1.8
Transverse normalized rms emittance [μm]	ε_n	25
Longitudinal emittance ($4\pi\ \sigma_E\ \sigma_T$) [eVs]	ε_l	0.314
Rms bunch length [mm]	σ_z	1.5
Relative rms energy spread [%]	p_T	0.1
Beta function at IP [mm]	β^*	1.5
Beam power with 10 Hz repetition rate [MW]	P_{beam}	14.4

Interaction Region

For the current designs of the IRs, the maximum allowed magnetic field at the beam envelope is assumed to be the 20 T and $L^* = 6$ m. A first design that includes only pure quadrupoles can be seen in Fig. 2a. The light blue boxes show the location and the length of the quadrupoles while their orientation shows the polarity (pointing upward/downward for positive/negative k_1). As the beta functions are increasing very fast right after the IP ($s = 0$), three short quadrupoles are used in this area in order to fully benefit from the maximum allowed magnetic field and reduce that way the length of the final focusing (FF) scheme. Each of these quadrupoles has different k_1 and their integrated strength is used to control the ratio between β_x and β_y at the end of the FF scheme. The last two quadrupoles (one defocusing and one focusing) are longer and are used for the point to parallel matching at the end of the FF scheme (optical $\alpha_x = \alpha_y = 0$). In Fig. 2a are also plotted with green line the linear dispersion (D_x) and with black line the beam envelope (half aperture) equal to $5\sigma + 2$ cm, where $\sigma = \max(\sigma_x, \sigma_y)$ and $\sigma_j = \sqrt{\varepsilon_j \beta_j + (D_j p_T)^2}$ with $j = x, y$. The extra 2 cm is the width of the magnets shielding. The maximum magnetic field at the beam envelope above defined (green circles), at $5\sigma_x$ (red squares) and at $5\sigma_y$ (blue triangles) are shown (right y-axis), respectively.

In the case where the magnets technology cannot reach 20 T in the near future, a lower field of 16 T can be used. For this latter case, similar IR designs with the 20 T ones can be used if one or a combination of the following modifications is performed: a) reduction of $\sqrt{s}$ to 8 TeV and increase of β^* (proportional to E^{-1}) and b) reduction of the aperture. With β^* inversely proportional to the energy, the divergence at the IP and the beam size for identical optics (similar k_1 magnets strength) becomes independent of energy. As a side effect of the first modification is the reduction of the integrated luminosity given that β^* is inversely proportional to the energy. Concerning the second approximation one can reduce the aperture by either reducing the beam envelope to $4\sigma + |D_x p_T| + 1.5$ cm with a minor effect on the luminosity (less than 1%) or by increasing the β^* by a factor ~2 (a bit larger than $(5/4)^2$).

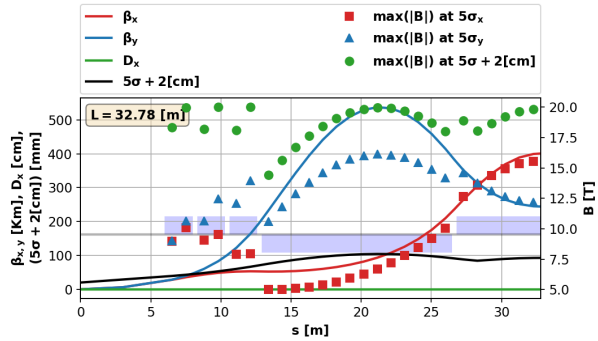

(a)

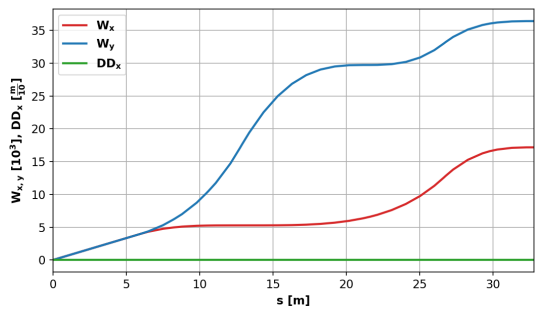

(b)

Figure 2: Evolution of a) the optical functions and the maximum magnetic field and b) the Montague chromatic functions in the right side of the final focusing scheme with only quadrupoles.

Alternative designs of the FF scheme that include dipole or combined function (dipole-quadrupole) magnets are developed to mitigate BIB by removing some of the decay products far enough from the detector and will be discussed in a future work.

Chromatic Correction Scheme

Due to the strong quadrupoles in the FF scheme (need for very small β^*) and the large energy spread ($p_T = 0.1\%$), the linear and non-linear chromatic phenomena are strong. More specifically the Montague chromatic functions ($W_{x,y}$) [12] that describe the optics mismatch of off-momentum particles w.r.t on-momentum ones are large as can be seen in Fig. 2b. For the compensation of such large W functions, a local chromatic correction (CC) scheme is developed right after the FF section in order to fully benefit from the large βs at that area. The maximum allowed magnetic field used for that lattice section is assumed to be the 16 T. One of the compact designs (large integrated sextupolar field) of the CC schemes is shown in Fig. 3a where the FF scheme is also included. In this plot the red, hashed blue and red+yellow color boxes

ISBN: 978-3-95450-227-1 ISSN: 2673-5490 doi:10.18429/JACoW-IPAC2022-MOPOTK031

indicate the dipole, dipole-quadrupole and dipole-sextupole magnets, respectively. The CC scheme include two sets of dipole-sextupole magnets (one acting on W_x and the other one on W_y) and are placed at positions where the β_x and β_y are maximum. Each set has two dipole-sextupole magnets separated by an identity like transformation (supported by the large βs) and with opposite normalized strength $(k_2, -k_2)$ in order to compensate the resonance driving terms (RDTs) excited by the dipole-sextupole. This design of the CC scheme differs from the ones proposed for other projects like the MAP and CLIC. The compensation of the W functions to almost zero value is presented in Fig. 3b.

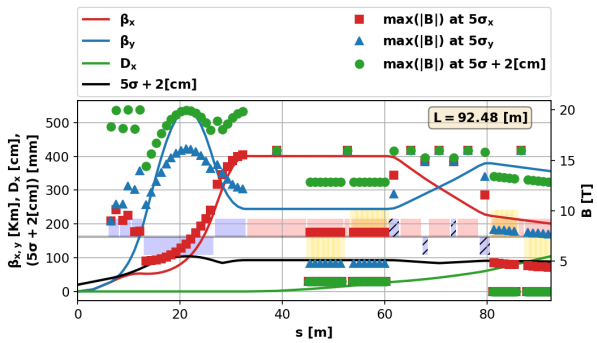

(a)

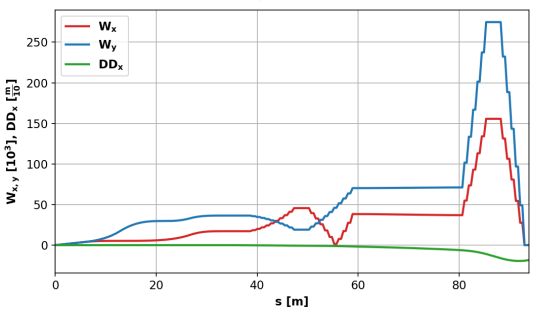

(b)

Figure 3: Evolution of a) the optical functions and the maximum magnetic field and b) the Montague chromatic functions in the right side of the final focusing scheme with only quadrupoles and the chromatic correction scheme.

Arc and Dispersion Suppressor

In the discussed lattice sections, strong dipolar components are located in regions with positive dispersion. Thus, the contribution to the momentum compaction factor (α_p) and the phase slip ($\eta_p \sim \alpha_p - 4.5\times10^{-10}$) are large. In order to keep the bunches short (small η_p), a negative contribution to α_p is needed and that is taking place in the arcs with a repeated use of flexible momentum compaction (FMC) cells [13]. With these FMC cells, the α_p, the 2π closing of the trajectory and the linear tune shift with energy in both transverse planes ($\xi_{x,y}$) are controlled with two sets of combined function dipole-sextupole magnets and the phase advance per FMC cell is $3\pi/2$ (-I transform every second cell). At the entrance and exit of each arc, dispersion suppressors are developed and once again the maximum magnetic field is assumed to be the 16 T. An early design of the right dispersion suppressor and the first FMC cells of the arc can be seen in Fig. 4 where the dipole-sextupole magnets are shown with yellow hashed color. For this design the optical functions at the entrance of the dispersion suppressor are not matched with the ones at the end of the CC scheme (shown in Fig. 3a).

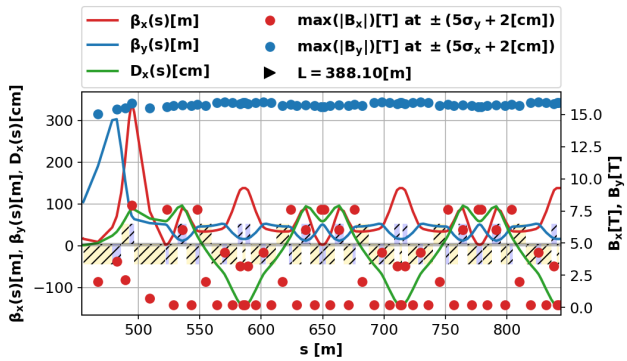

Figure 4: Evolution of the optical functions and the maximum magnetic field in the dispersion suppressor and the first arc cells.

CONCLUSION

Muon colliders are proposed for high energy lepton collisions in a high magnetic field ring without large synchrotron radiation losses. Due to the unstable nature of the muons, different challenges had to be addressed leading to novel design concepts for the collider ring. In this work, the current designs of the basic building blocks, final focusing section, chromatic correction section and arc lattices cell of the $\sqrt{s}$ = 10 TeV muon collider ring are presented. Given the need for small circumference and β^* values, the requirement to cope with radiation caused by neutrinos as well the presence of strong chromatic phenomena, high magnetic fields and dipolar components are extensively used in these designs. The CC scheme developed to control the optics aberrations after the FF scheme is different from other optics proposals requiring local chromaticity compensation. The control of the bunch length (through the momentum compaction factor) and the linear tune shift with energy is performed in the arcs with the FMC cells.

ACKNOWLEDGEMENTS

Special thanks to Dr. Katsunobu Oide and Dr. Rogelio Tomas for the fruitful discussions we had on the collider ring design.

REFERENCES

[1] O. S. Brüning *et al.*, "LHC Design Report", CERN, Geneva, Switzerland, Rep. CERN-2004-003-V-12004, 2004.

[2] I. Zurbano Fernandez *et al.*, "High-Luminosity Large Hadron Collider (HL-LHC): Technical design report", CERN, Geneva, Switzerland, Rep. CERN-2020-01, Dec. 2020.

ISBN: 978-3-95450-227-1 ISSN: 2673-5490 doi:10.18429/JACoW-IPAC2022-MOPOTK031

[3] D. Schulte, "The International Muon Collider Collaboration", in *Proc. IPAC'21*, Campinas, Brazil, May 2021, pp. 3792–3795. doi:10.18429/JACoW-IPAC2021-THPAB017

[4] M. Benedikt *et al.*, "Future Circular Collider - European Strategy Update Documents", CERN, Geneva, Switzerland, Rep. CERN-ACC-2019-0007, Jan. 2019.

[5] T.K. Charles *et al.*, "The Compact Linear Collider (CLIC) - 2018 Summary Report", doi:10.48550/arXiv.1812.06018, May 2019.

[6] F. Tikhonin and G. Budker, "On the effects with muon colliding beams", JINR Report P2-4120, p. 33–39, 1968.

[7] M. A. Palmer, "The US muon accelerator program", doi:10.48550/arXiv.1502.03454, Feb. 2015.

[8] MICE collaboration, "Demonstration of cooling by the Muon Ionization Cooling Experiment", *Nature*, vol. 578(7793), pp. 53–59, 2020. doi:10.1038%2Fs41586-020-1958-9

[9] D. Alesini, "Positron driven muon source for a muon collider", doi:10.48550/arXiv.1905.05747, May 2019.

[10] D. Stratakis *et al.*, "A Muon Collider Facility for Physics Discovery", doi:10.48550/arXiv.2203.08033, Mar. 2022.

[11] N. Bartosik *et al.*, "Simulated Detector Performance at the Muon Collider", doi:10.48550/arXiv.2203.07964, Mar. 2022.

[12] B. W. Montague, "Linear Optics For Improved Chromaticity Correction", CERN, Geneva, Switzerland, Rep. CERN-LEP-Note-165, 1979.

[13] S. Y. Lee, K. Y. Ng, D. Trbojevic, "Minimizing dispersion in flexible-momentum-compaction lattices", *Phys. Rev. E*, vol. 48, p. 3040, Oct. 1993. doi:10.1103/PhysRevE.48.3040